Measurements of domain-wall energy density for amorphous rare earth–transition metal thin films

R. A. Hajjar[a] and H-P. D. Shieh
IBM Research Division, T. J. Watson Research Center, Yorktown Heights, New York 10598

(Received 30 March 1990; accepted for publication 21 June 1990)

The value of domain-wall energy density (σ_w) has been most often assumed to be proportional to $\sqrt{A_x K_u}$, where exchange stiffness (A_x) is usually calculated from the mean-field theory. We report a simple method to derive σ_w from the difference between the onset of expanding and collapsing fields (ΔH) for circular domains. A micro-Kerr hysteresis-loop tracer with submicrometer resolution is used to measure the destabilizing field of domains written thermomagnetically in TbFeCo and GdTbFeCo films.

I. INTRODUCTION

Domain-wall energy density (σ_w) plays a critical role in the stability and regularity of the thermomagnetically written domains in rare earth–transition metal (RE-TM) thin films. Based on the classical micromagnetic theory,[1] σ_w is found to be proportional to $\sqrt{A_x K_u}$, where A_x is the exchange stiffness derived from the mean-field theory or other methods (neutron scattering, for example) and K_u is the uniaxial anisotrophy constant found usually by a torque magnetometry. However, it was found that non-*s*-state rare-earth elements such as Tb and Dy in RE-TM materials are responsible for the occurrence of random axis anisotropy and could be characterized with more than one uniaxial anisotropy constant.[2] In the absence of a reliable model of the complex domain-wall structure, it has been proposed[3] to derive the domain-wall energy density from experimental observations. The method consists of measuring the difference of expanding and collapsing fields for micrometer-size domains. In this paper, we report measurements of the domain-wall energy density for TbFeCo and GdTbFeCo magneto-optical (MO) recording media.

II. THEORY

In MO materials there are three contributions to the energy of formation of the domain[4]: the external energy, the domain-wall energy, and the magnetostatic (demagnetizing) energy. The forces on the domain wall may then be calculated by differentiating the corresponding energy with respect to the domain radius.

Consider a uniformly magnetized RE-TM sample of net magnetization M_s with a domain of radius R and thickness h. Assuming the wall width is much smaller than the film thickness, the external force per unit area applied on the domain wall due to an external field H perpendicular to the sample is given by

$$F_{\text{ext}} = 2M_s H. \tag{1}$$

We will adopt a negative sign for an inward force acting on the domain.

The demagnetizing energy was found to be proportional to $2\pi M_s^2$ times a complex function of thickness and domain radius. For a thin domain wall of large radius compared to the film thickness a good estimate of self-magnetic energy per unit area of domain wall is given by[4]

$$\Delta E_{\text{dmag}} \simeq 6\pi h M_s^2. \tag{2}$$

Consequently F_{dmag} is outward with an approximate magnitude

$$F_{\text{dmag}} = 6\pi h M_s^2 / R. \tag{3}$$

The domain-wall energy arises from a combination of the anisotropy and exchange energy. A simple way to derive F_{wall} is by considering a domain which shrinks from a radius R to a radius $R - \Delta$. The net change in energy is

$$\Delta E_{\text{wall}} = 2\pi(R-\Delta)h\sigma_w - 2\pi R h \sigma_w = F_{\text{wall}}(2\pi R h)\Delta. \tag{4}$$

The wall force per unit wall area is then

$$F_{\text{wall}} = -(\sigma_w / R). \tag{5}$$

Note the F_{wall} is always inward, trying to collapse the domain. Finally, the total force acting on a domain is given by

$$F_{\text{tot}} = \pm F_{\text{ext}} + F_{\text{dmag}} - F_{\text{wall}}. \tag{6}$$

When a threshold field $H = H_1$ is applied to expand the domain the total outward force becomes equal to the coercivity force F_c. Similarly, at the threshold of collapse (i.e., $H = H_2$) the total force will be inward and equal to $-F_c$.

Consequently the total forces in the case of expansion and collapse are as follows:

$$\text{Expansion:} \quad F_c = F_{\text{ext}(H_1)} - F_{\text{wall}} + F_{\text{dmag}}; \tag{7}$$

$$\text{collapse:} \quad -F_c = -F_{\text{ext}(H_2)} - F_{\text{wall}} + F_{\text{dmag}}. \tag{8}$$

Summing Eqs. (7) and (8) we obtain

$$F_{\text{wall}} = \frac{F_{\text{ext}(H_1)} - F_{\text{ext}(H_2)}}{2} + F_{\text{dmag}}. \tag{9}$$

Therefore, the domain-wall energy density can be found by substituting the expressions of the forces derived above:

$$\sigma_w = 6\pi h M_s^2 + M_s R(H_1 - H_2). \tag{10}$$

It is important to note that the formulation of the domain-wall energy density shown in Eq. (10) holds only for simple circular walls and does not take into account Bloch lines or

[a] Permanent address: Optical Science Center, University of Arizona, Tucson, AZ 85721.

 0021-8979/90/204199-04$03.00

Bloch points. In that case, the expression for the domain wall energy density for circular domains becomes[5]

$$\sigma_w \simeq 4\nu^{-1}(K_u R + n_0^2 A_x/R), \tag{11}$$

where n_0 is the number of Bloch lines and ν is given by

$$\nu = \left[n_0^2 + (R/\sqrt{A_x/K_u})^2\right]^{1/2}, \tag{12}$$

with the assumption that the domain radius R is much larger than the domain wall width $\sqrt{A_x/K_u}$. In the limit of $n_0 = 0$, Eq. (11) reduces to the standard formula for domain-wall energy density discussed earlier. Equation (11) simply implies that σ_w increases as the number of Bloch lines increases. For the sake of comparison assume a 1-μm-size domain with $K_u = 10^6$ erg/cm^3 and $A_x = 10^{-7}$ erg/cm, we find $\sigma_w = 1.265$ erg/cm^2 for $n_0 = 10$ and $\sigma_w = 1.267$ erg/cm^2 for $n_0 = 10$ Bloch lines.

When the effect of Bloch lines on the demagnetizing energy is taken into account, Eq. (2) should be rewritten as

$$\Delta E_{\text{dmag}} = 2\pi h M_s^2 G(\Lambda,\rho_0,n_0), \tag{13}$$

where $G(\Lambda,\rho_0,n_0)$ is a complicated function of $\Lambda = \lambda/h$, $\rho_0 = R/h$, and n_0. For the case of $n_0 = 1$, it was shown[6] that as Λ approaches zero, the function $G(\Lambda,\rho_0,n_0)$ approaches a constant value of 3.

We now investigate the effect of Bloch lines on the demagnetizing energy using the fast Fourier transform technique as described in Refs. 6 and 7. Assume a reverse magnetized circular domain of radius R with n_0 Bloch lines on a 256×256 discrete hexagonal lattice of unit spacing d. The reduction in demagnetizing energy per unit wall area, caused by the creation of a domain, is obtained by subtracting the shape energy term ($2\pi M_s^2$) from the magnetostatic energy term and then normalized by the perimeter of the domain, namely

$$\Delta E_{\text{dmag}} \simeq (2\pi h M_s^2 - E_{\text{dmag}})(A/2\pi R), \tag{14}$$

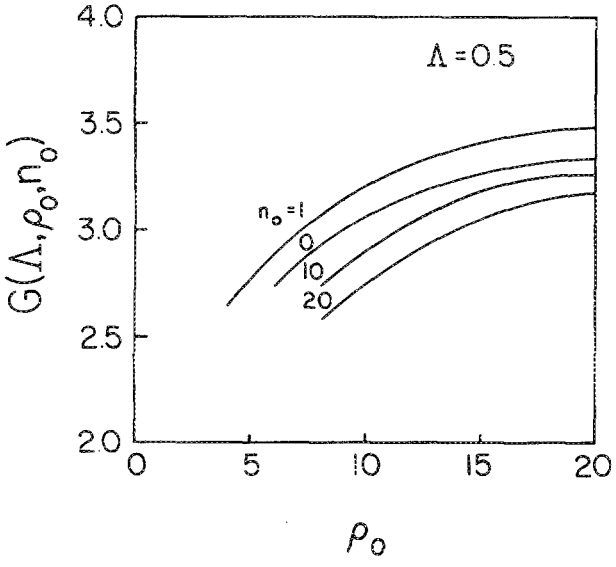

FIG. 1. $G(\Lambda,\rho_0,n_0)$ as functions of ρ_0 and n_0 at $\Lambda = 0.5$. $G(\Lambda,\rho_0,n_0)$ is a function used to calculate demagnetizing energy in perpendicular oriented magnetic thin films.

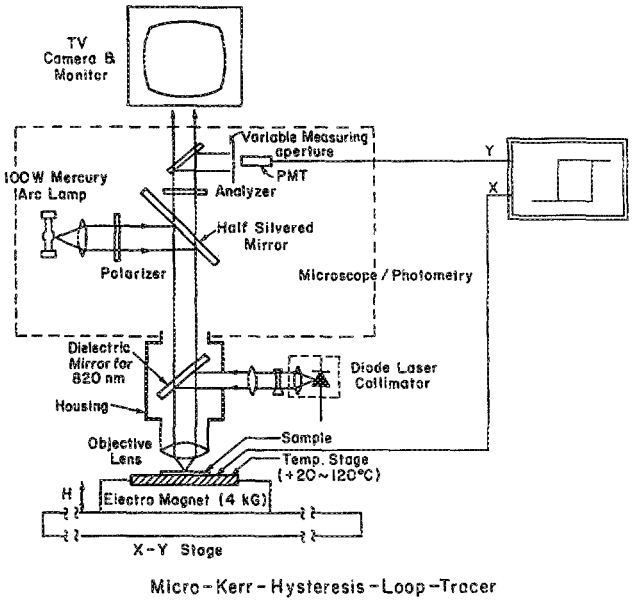

FIG. 2. Schematic diagram of the micro-Kerr hysteresis-loop tracer with submicrometer spatial resolution.

here A is the area of the film. In this case $A = 256d \times 256d$. $G(\Lambda,\rho_0,n_0)$ is found by comparing Eq. (13) with Eq. (14). Figure 1 is a plot of $G(\Lambda,\rho_0,n_0)$ as a function of ρ_0, and n_0 at Λ of 0.5. For $R = 1\ \mu$m, $h = 100$ nm ($\rho_0 = 10$), $G(\Lambda,\rho_0,n_0)$ varies between 2.8–3.2 for $n_0 = 20$ to $n_0 = 1$. This change corresponds to $\sigma_w = 1.44$ to 1.5 erg/cm^3 for $M_s = 50$ emu/cm^3 and $\Delta H = 200$ Oe. In most RE-TM thin films, Λ is about 0.05. In that case, a variation of $G(\Lambda,\rho_0,n_0)$ as a function of n_0 is even smaller. From these results we conclude that the effect of Bloch lines can be neglected in the calculation of σ_w from Eq. (10) since a $\pm$ 10% error in the measurements is expected.

III. EXPERIMENTAL PROCEDURE

In order to measure fine variations of collapsing and expanding fields for micrometer-size domains, a magneto-optical hysteresis loop tracer with submicrometer spatial resolution is used.

The micro-Kerr hysteresis-loop tracer, shown schematically in Fig. 2, is described elsewhere.[6] A 30-mW laser diode coupled into the objective of the microscope is used for writing micrometer-size domains. The MO signal is detected by a photomultiplier tube (PMT) with a variable measuring aperture. Figure 2(a) is a photograph of a thermomagnetically written domain (in black contrast) and an image of the 1-μm measuring aperture (in white contrast). Then position the magnetic domain within the measuring aperture. The PMT only senses the light from the demagnified spot on the sample surrounding the domain [Fig. 3(b)]. Samples are placed on a heating stage with temperature range of 20–200 °C and a 4-kOe electromagnet is used to destabilize the domains. An x-y recorder plots the MO signal from the PMT versus applied magnetic field.

To determine the critical expanding and collapsing fields, a micrometer-size domain is written initially onto the

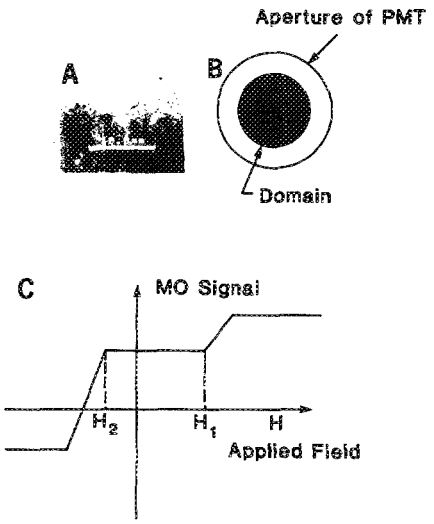

FIG. 3.(a) A photograph of a thermomagnetically written domain (in black contrast) and the image of the 1-μm measuring aperture. (b) Domain imaged by a measuring aperture. (c) Plot of MO signal from PMT vs applied magnetic field. H_1 and H_2 are the onset of expansion and collapse magnetic fields, respectively.

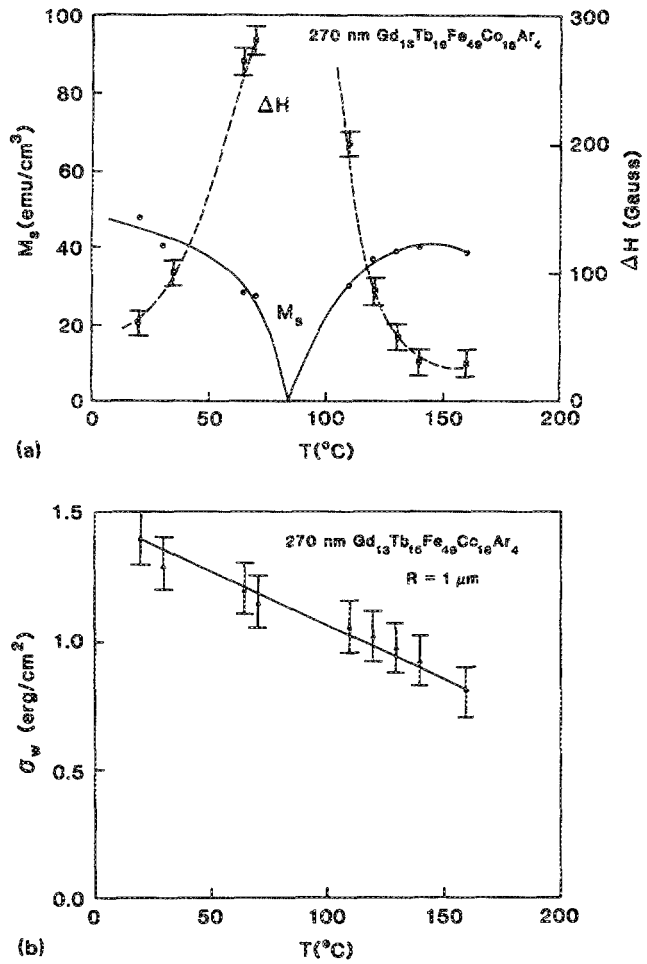

FIG. 4.(a) M_s (—) and ΔH (--) vs temperature. (b) σ_w vs temperature for a 270-nm-thick $Gd_{13}Tb_{16}Fe_{49}Co_{18}Ar_4$ sample.

sample. A magnetic field is applied in order to expand the domain. At the onset of expansion, at an applied field H_1, the MO signal starts increasing [Fig. 3(c)] until it reaches a steady state which corresponds to a domain greater than the size of the measuring aperture. The same applies when measuring the collapsing field except that after rewriting the domain, the magnet is switched to the opposite direction. The critical collapse field is then H_2 [Fig. 3(c)].

The processes are repeated for the same sample at different temperatures for one to four micrometer-size domains in TbFeCo and GdTbFeCo samples with various thicknesses and compositions.

IV. EXPERIMENTAL RESULTS AND DISCUSSION

Figure 4(a) shows M_s and ΔH ($H_1 - H_2$) versus temperature for a 270-nm $Gd_{13}Tb_{16}Fe_{49}Co_{18}Ar_4$ sample with a 100-nm SiO_2 overcoat. The sample has a coercivity (H_c) of 3 kOe at room temperature, a compensation temperature (T_{comp}) and Curie temperature (T_C) of 85 and 320 °C, respectively. The corresponding values of σ_w derived from Eq. (10) are plotted versus temperature for 1-μm domains in Fig. 4(b). Note that σ_w decreases linearly as temperature increases while ΔH diverges around 85 °C. Linear decreasing of σ_w with temperature is correlated with the temperature dependence of $\sqrt{A_x K_u}$.[4] The shape of $\Delta H(T)$ is very similar to $H_c(T)$ where both diverge at T_{comp} near which σ_w is the dominant force acting on the domain wall. In the same sample (Fig. 5) and at room temperature, it is found that ΔH decreases as the domain spot size increases, while σ_w is almost constant. The variations of σ_w are assumed to be due to experimental errors which have been accounted for by calculating the standard deviation for every set of measurement. It is important to note that in the calculations of σ_w we have assumed a $\pm$ 10 G error in ΔH, a $\pm$ 0.1 μm error in R,

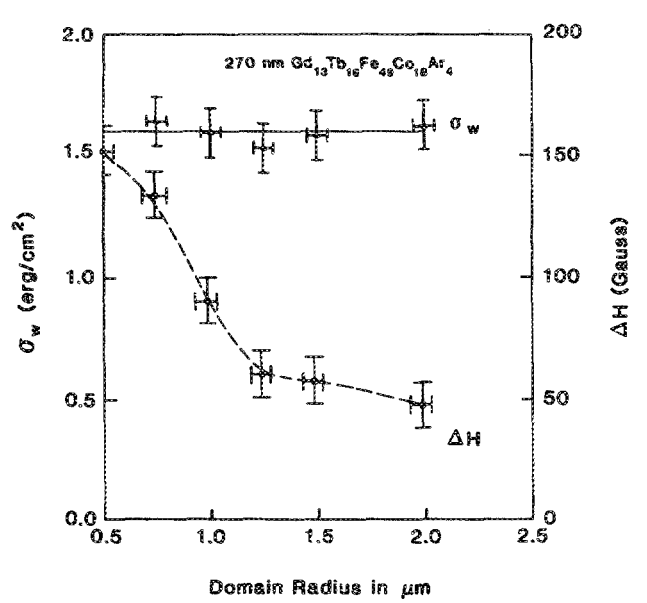

FIG. 5. σ_w (—) and ΔH (--) vs domain radius for a 270-nm-thick $Gd_{13}Tb_{16}Fe_{49}Co_{18}Ar_4$ sample at room temperature.

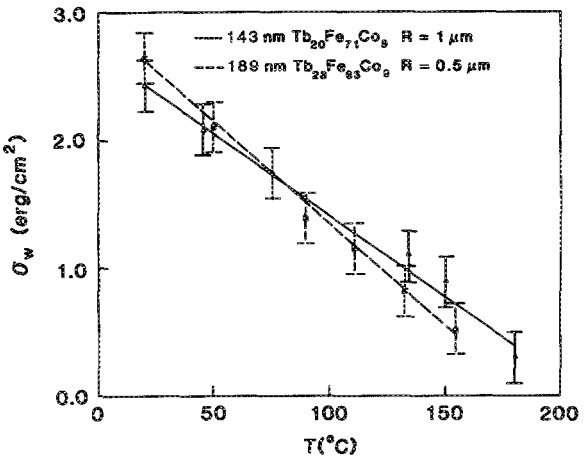

FIG. 6. σ_w vs temperature for a (--) $Tb_{28}Fe_{63}Co_9$ and a (—) $Tb_{20}Fe_{71}Co_9$ sample.

and errors up to 10% in M_s which also accounts for the error in thickness.

Figure 6 shows σ_w versus temperature for two TbFeCo samples. The same linear decrease of σ_w toward T_C is observed. The first sample, 189-nm-thick $Tb_{28}Fe_{63}Co_9$, has an H_c of 2.7 kOe at room temperature and a T_C of 190 °C. For this sample ΔH is negative (i.e., the collapsing field is larger than the expanding field) implying a large demagnetizing energy. The second sample, 143-nm-thick $Tb_{20}Fe_{71}Co_9$, has an H_c of 2.9 kOe at room temperature and a T_C of 210 °C. It is worthwhile to mention that this sample ($Tb_{20}Fe_{71}Co_9$) exhibits irregular domain patterns during expansion. Nevertheless, the model is able to predict σ_w since it only considers the difference between the expansion and collapse fields. Therefore, small irregularities in the domain wall will cancel out.

The torque magnetometer measured K_u for $Tb_{20}Fe_{71}Co_9$ at room temperature is 1.7×10^6 erg/cm^3. Assuming $\sigma_w = 4\sqrt{A_x K_u}$, and using the obtained σ_w of 2.43 erg/cm^2, the exchange stiffness A_x for the $Tb_{20}Fe_{71}Co_9$ at room temperature is derived to be 2.17×10^{-7} erg/cm. The derived A_x is similar to the mean-field calculated A_x for $(Tb_{21}Fe_{79})_{95}Ar_5$.[7] σ_w for the TbFeCo samples at room temperature is about a factor of 2 larger than that in the GdTbFeCo, where σ_w is about 1.4 erg/cm^2, although the Curie temperature of the latter is much higher than that of the former. This is in agreement with the dependence of σ_w on K_u which is smaller in the case of GdTbFeCo due to the dilution of strong single-ion anisotropy by the *s*-state Gd atoms.

V. CONCLUSION

Domain-wall energy density was measured as a function of radius, temperature, and composition using a micro-Kerr hysteresis-loop tracer with submicrometer spatial resolution. It has been found that σ_w is a weak function of domain size and a linear decreasing function of temperature. Room-temperature σ_w of $Tb_{28}Fe_{63}Co_9$ is 2.66 erg/cm^2, which is almost a factor of 2 higher than that of GdTbFeCo, indicating the dilution of single-ion anisotropy by Gd constituent. As uniaxial anisotropy constant K_u can be measured by a torque magnetometer, exchange stiffness A_x can then be derived. For the $Tb_{20}Fe_{71}Co_9$ film, the derived A_x at room temperature is 2.17×10^{-7} erg/cm. This simple method is applicable to derive domain-wall energy density and exchange stiffness and their temperature dependences in MO recording materials.

ACKNOWLEDGMENTS

The authors would like to thank Professor Masud Mansuripur of the Optical Sciences Center for helpful comments and criticism. One of us (R.A.H.) would like to acknowledge the support of an IBM Fellowship.

[1] A. P. Malozemoff and J. C. Slonczewski, *Magnetic Domain Walls in Bubble Materials* (Academic, New York, 1979).
[2] R. A. Hajjar, F. L. Zhou, and M. Mansuripur, J. Appl. Phys. **67**, 5328 (1990).
[3] M. Mansuripur, J. Appl. Phys. **66**, 6175 (1989).
[4] M. Mansuripur, and G. A. N. Connell, J. Appl. Phys. **55**, 3049 (1984).
[5] M. Mansuripur, J. Appl. Phys. **63**, 5089 (1988).
[6] M. Mansuripur, J. Appl. Phys. **66**, 3731 (1989).
[7] M. Mansuripur, IEEE Trans. Magn. **MAG-24**, 2326 (1988).
[8] H-P. D. Shieh and M. H. Kryder, IEEE Trans. Magn. **24**, 2464 (1988).
[9] M. Mansuripur and M. F. Ruane, IEEE Trans. Magn. **MAG-22**, 33 (1986).